Bull. Tokyo Univ. For., 80, 37-68 (1988)

Warping in New Crop Radiata Pine 100 × 50 mm (2 by 4) Boards

Akiyoshi MISHIRO* and Rudolf E. BOOKER**

Table of Contents

1. Introduction

Warping of timber during drying causes significant economic losses. Because timber is an anisotropic material it is impossible to eliminate warp completely. However it can be reduced by using correct sawing and drying practices. Unfortunately, boards sawn from young, small diameter radiata pine logs show substantial drying degrade even when correct drying practices are used (MACKEY and RUMBALL 1971, Haslett and McConchie 1986).

* Department of Forest Products, Faculty of Agriculture, The University of Tokyo.
東京大学農学部林産学科
** Senior Scientist, Product Development Group, Wood Technology Division, Forest Research Institute, Ministry of Forestry, Rotorua, New Zealand.
ニュージーランド森林省森林研究所木材部

The anatomical characteristics of wood near the pith (juvenile or core wood) differ from those of more mature wood (SHELLY *et al.* 1979). The corewood has relatively high longitudinal shrinkage, high spiral grain angle, large fibril angle and is also more likely to have compression wood than wood from the exterior of the tree. Obviously corewood also possesses a greater number of knots. More efficient utilisation of young, small diameter radiata pine logs and the core wood of mature logs could be achieved if warp-prone materials could be separated prior to drying. To achieve this goal it is necessary to understand the mechanism of warping and to identify the wood characteristics that cause it. Although it has been the subject of many investigations it has proved extremely difficult to obtain a good relationship between warp and its causative factors (KLOOT and PAGE 1959, DU TOIT 1963, and BALODIS 1972).

The purpose of this study is to identify and if possible to quantify the relationship between warp and the anatomical and physical properties of new crop radiata pine timber. Consequently the following parameters were measured for a series of boards: (1) bow, (2) crook, (3) twist, (4) mean width of the annual rings, (5) orientation of the annual rings with respect to the board surfaces, (6) distance from the pith, (7) grain deviation, (8) basic density, (9) the position and size of the knots and lastly, (10) the inclusion of pith.

The dependence of bow, crook and twist of the boards was then related to the other board parameters.

2. Material and Preparation

2.1 Log selection

Four logs each 5.7 m long were obtained from Kaingaroa Forest. They were selected for minimal sweep and taper, absence of compression wood and uniform circular cross-section with the pith located in the centre. The logs were transported to the Timber Industry Training Centre (TITC) near Rotorua and the diameter, branch index, sweep and the number of annual rings of each log were measured. Their properties are given in Table 1. Discs 300 mm in length were cross-cut from both ends of each log for the measurement of the radial distribution of spiral grain and shrinkage. A different colour was sprayed on both ends of each log, and a mark was put on the annual rings at 5 ring intervals from the pith and distance from the pith to every fifth ring position was measured.

2.2 Conversion of the logs

All logs were sawn into boards 100 by 50 mm in cross section (about 5.0 m in length) by taper sawing and all boards were dressed at the Timber Industry Training Centre. Seventy-six boards were obtained and transported to the Forest Research Institute.

2.3 Sampling

A leading edge was marked with a marker pen on all boards. The leading edge is the

Table 1. Log properties

Log Number	Number of annual rings	Butt end diameter under bark (mm)	Top end diameter under bark (mm)	Sweep (mm)	Branch index (mm)
1	30	431	416	4.0	32.5
2	33	388	381	2.5	25
3	34	524	510	12.5	55
4	34	553	526	1.5	56

Note: The logs were 5.7 m long.

edge of the board that was closest to the centre of the log prior to sawing (Fig. 1). This edge and its adjacent planes were used as a reference for all measurements.

Reference, moisture content and grain deviation specimens were taken from both ends of each board as shown in Figure 2. The reference and grain deviation specimens were stored in a refrigerator. The 4.8 m long boards were anti-sapstain dipped and stored in block stack wrapped in plastic until they were dried. The moisture content specimens were placed in a plastic bag immediately after cutting to prevent drying out and weighed within two hours. Their volume was determined by the immersion and upthrust method.

2.4 Methods of measurement

(a) Annual ring orientation (θ) and distance from the pith (r)

The distance from the pith (r) and the annual ring orientation (θ) were measured for all the reference specimens cut from both ends of the 76 boards (cf. Fig. 2) by the overlay method (BOOKER, 1987), as well as by direct measurement. Because, as described above, each log was colour coded at its ends, the board ends could be assembled after sawing into the log shape and r and θ could hence be measured directly. Sixty-one boards were selected for study to give a good selection of r and θ. Measurements of angle were always taken looking along a board from the butt end.

(b) Grain deviation

The grain angle specimens cut from the boards were cleaved along the grain at 10 mm intervals with a cleaver held parallel to the annual rings. This created true tangential/longitudinal (TL) surfaces for which the spiral grain angle was measured. The grain direction was measured by scribing the tangential surface with a needle using a swivel-handled scriber (BS 4978). The average grain angle for each specimen as well as the standard deviation were calculated. In a tree or board the grain deviation spirals either to the right or to the left. The two types are called Z- or negative spiral grain and S- or positive spiral grain and they are defined in Figure 3. Grain deviation was measured in the green condition.

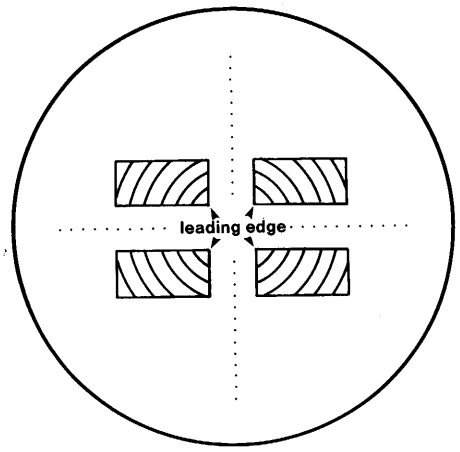

Fig. 1. The leading edge of boards.

A diametral strip 50 mm wide and 50 mm along the grain was taken from each 300 mm long disc to measure the radial distribution of spiral grain. From the bark side, successive rings were split off with a cleaver at the ear-

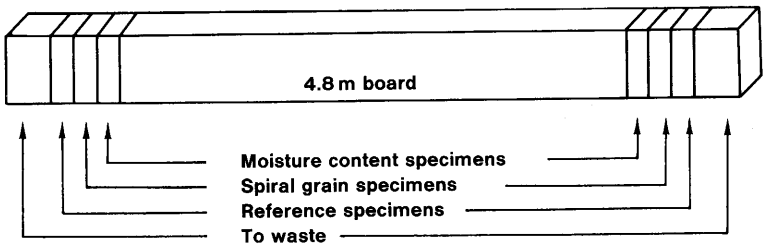

Fig. 2. Diagram showing the method of cutting each 4.8 m board, and the reference, spiral grain and moisture content (basic density) specimens.

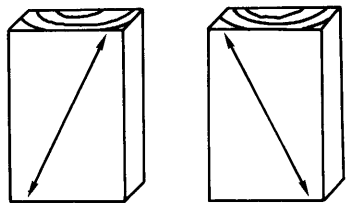

Fig. 3. Definition of grain direction.

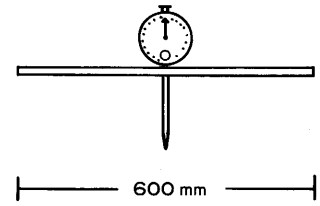

Fig. 4. Instrument to measure over a 600 mm length the crook and bow contributed by individual knots or whorl of knots.

lywood/latewood boundary. The grain angle of each exposed tangential surface was measured with a scriber in the usual way. The grain angle of each annual ring was taken to be the average of the spiral grain angle of the ring on the two diametrically opposite sides of the tree.

(c) Percentage saturation of the wood

The percentage saturation of the wood was calculated from the moisture control specimens using the formula:

$$\% \text{ saturation} = \frac{\text{actual moisture content}}{\text{maximum possible moisture content}} \times 100\%$$

$$= mc \times \left(\frac{1}{\rho} - \frac{1}{ws\rho}\right)^{-1} \times 10^{-3}\% \text{ (MKS units)}$$

where ρ = basic density

$ws\rho$ = wood substance density (1520 kg/m^3)

The basic (oven-dry) density of the specimens was determined in the normal manner.

(d) Heartwood content

The boundary between heartwood and sapwood can be easily distinguished by colour in fresh green radiata pine wood. The heartwood content as a percentage of the cross-section was measured on the reference specimens.

(e) Shrinkage

From each disc a diametral slab was sawn 60 mm wide by 170 mm along the grain. This was sawn into a series of shrinkage specimens 50×50 mm in cross-section and 150 mm along the grain, so that a series of shrinkage specimens was created extending from the pith to the outer sapwood. The endfaces were coated with paraffin and the centres of all six planes were identified and the dimensions measured. The specimens were air-dried to 12% moisture content. The shrinkage was calculated as a function of radial position and annual ring number.

(f) Warp

All measurements of warp were done in the usual way and taken to the nearest mm. Twist measurements were made at the top end of each board. The crook and bow caused by an individual knot or whorl of knots was measured with the instrument shown in Figure 4. It was used to measure the distortion caused by the knot(s) over a distance of 600 mm.

2.5 Pre-drying observations and measurements on the 4.8 m boards.

For the sixty-one green boards the following variables were measured or recorded:

(a) The boundary between heartwood and sapwood was marked on the boards and lines were drawn at 1 m intevals from the butt end.

(b) All knots in each board were numbered and it was recorded where each knot

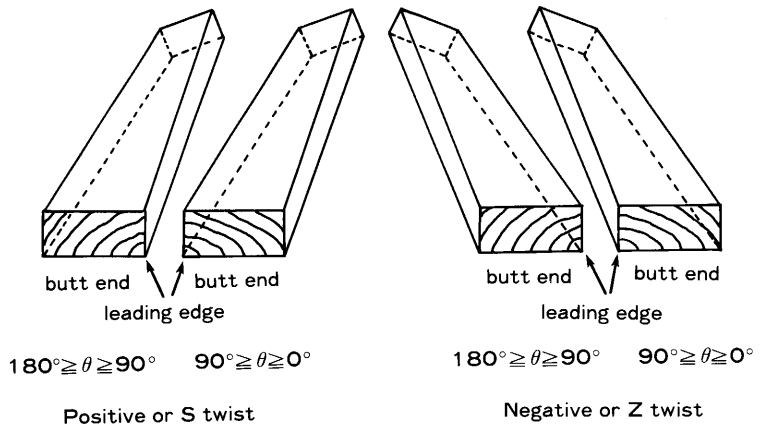

Fig. 5. Sign convention for twist.

reached the surface.

(c) For each knot the size and the area of the grain distortion around it were traced on translucent paper. This gives a complete record of the position and size of the knots in each board, as the distances to the leading edge and the butt end can be measured readily from the tracings.

(d) Green weight, length as well as thickness and width at 1 m intervals.

(e) The overall warp of the boards as well as the warp caused by each whorl of knots.

(f) Position of maximum warp.

2.6 Drying

After all measurements on the green 4.8 m boards had been completed, the sixty-one boards were kiln dried with no constraint whatsoever for 24 days at a dry-bulb temperature of 45℃ and a wet-bulb temperature of 35℃ (RH=44%, EMC=7%). During the drying, warp and weight of the boards were recorded three times. After drying was completed the final steps were carried out:

(a) The boards were weighed and the length as well as the thickness and width were determined at 1 m intervals.

(b) The warp of the boards was determined as well as the position along the board where it was a maximum.

(c) The warp introduced by each whorl of knots or single knot over a distance of 600 mm was measured for all boards.

(d) Boards were selected for which over an interval of 2.4 m the distortion was not affected by the presence of knots. The distortion was measured.

(e) Kinks were examined.

(f) Photographs were taken.

After all measurements on the 4.8 m board had been completed, reference, moisture content and grain deviation specimens were cut from the dry boards at 1 m intervals.

3. Sign conventions

Previous investigators have always measured crook, bow, and twist on whichever side of a board it was found, which meant that warp was always positive or absent. In this article we are not only concerned which the magnitude of degrade, but also its direction, so

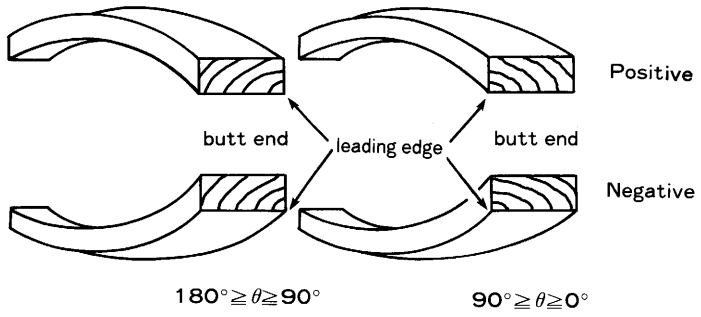

Fig. 6. Sign convention for bow.

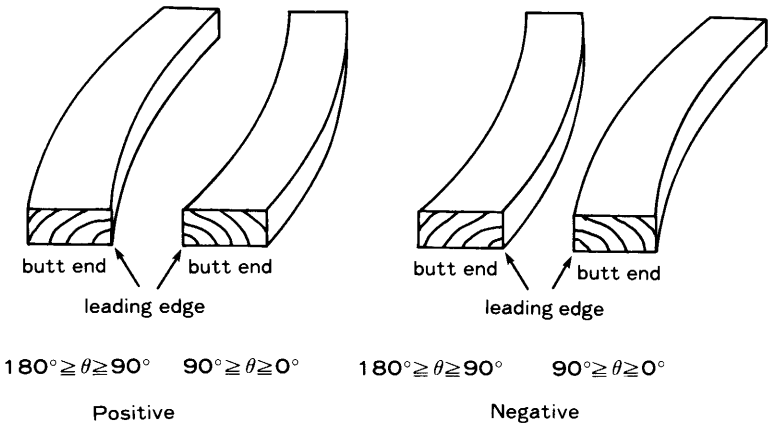

Fig. 7. Sign convention for crook.

that degrade can be either positive or negative. Consequently the direction of degrade in a boards has to be uniquely defined. The concept of a leading edge in boards has already been introduced in section 2.3 and Figure 1. The two board surfaces that contain the leading edge are the surfaces with respect to which twist, bow and crook are measured. The sign convention for twist is as follows. If the right hand side of the top of a board is raised (Fig. 5), positive or S-twist is said to occur. Similarly, if the left hand side of the top of the board is raised, the twist is negative or Z-twist.

The sign convention for bow is shown in Figure 6. If the wide board surface containing the leading edge is convex the board is said to possess negative bow. If it is concave, bow is said to be positive.

The sign convention for crook is shown in Figure 7. If the narrow board surface containing the leading edge is convex crook is considered to be negative, while if it is concave crook is positive.

4. Results and Discussion

4.1 The range of board (r, θ) values

Figure 8 shows a graph of r versus θ for the centroids of the boards used. It shows that practically the full range of board coordinates was covered. At the start of the experiment some boards with identical coordinates were eliminated to avoid duplication of effort.

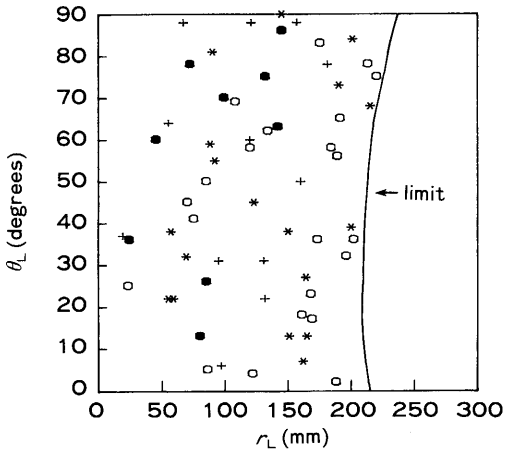

Fig. 8. Graph of θ_L versus r_L for 61 boards in this experiment. The limit line indicates the maximum theoretical r_L value at a given θ_L that can be sawn from the largest diameter log (no. 4). The graph indicates that an excellent spread of values was achieved. r_L: average distance from the centroid of the two end cross-sections of each board to the pith, as measured in the log assemble. θ_L: average annual ring angle co-ordinate for the two end cross-sections of each board, as measured in the log assemble. +, Log 1; ●, Log 2; ∗, Log 3; ○, Log 4.

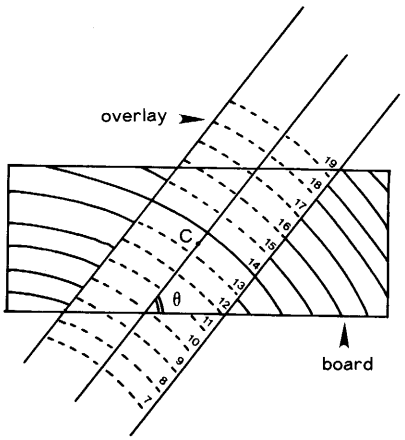

Fig. 9. Use of an overlay to determine the coordinates of the centroid. The arcs on the transparent overlay are shown hatched, the annual rings solid. In this example the 150×60 mm board has coordinates $r=135$ mm, $\theta=54°$ (from BOOKER R. E., 1987).

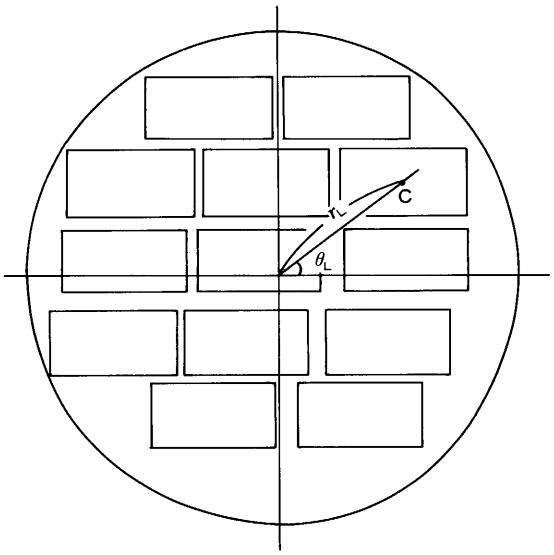

Fig. 10. Schematic diagram of the sawing of the logs and the measurement of the in-log (r_L, θ_L) coordinates for each board. C: centroid of the board.

4.2 Comparison of annual ring coordinates obtained by different methods

The radius of curvature and the orientation of the annual rings (r_0, θ_0) in each board were determined at the centroid of the cross-cut surfaces of the reference specimens of each board with Booker's overlay method (BOOKER, 1987). This method is shown in Figure 9. In addition, the in-log coordinates (r_L, θ_L) were measured as shown in Figure 10, where r_L is the

Table 2. The under bark radius of the discs in the four quadrants of each log

Tree No. and disc name		Radius from bark to pith centre (mm)			
		N	S	W	E
1	top	215	186	212	188
	butt	226	225	245	208
2	top	176	184	170	191
	butt	191	204	200	201
3	top	—	—	—	—
	butt	236	285	287	236
4	top	290	222	270	245
	butt	302	257	276	256

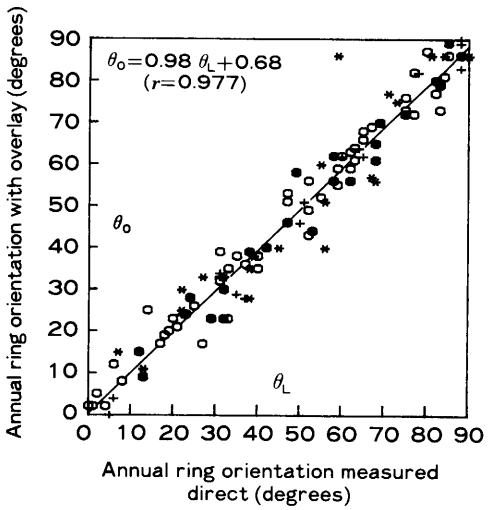

Fig. 11. Relationship between the annual ring orientation measured with an overlay (θ_0) and in the log (θ_L). +, Log 1; ●, Log 2; ∗, Log 3; ○, Log 4.

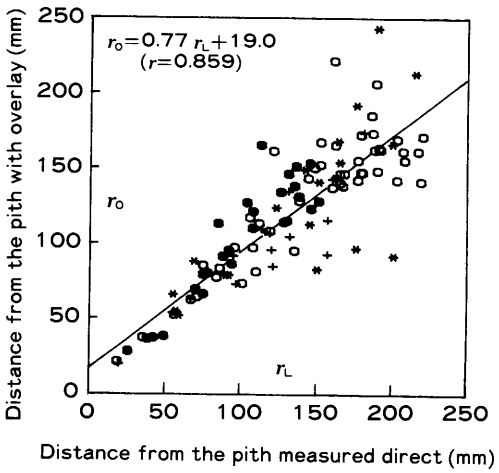

Fig. 12. Relationship between distance from the pith measured with an overlay (r_0) and in the log (r_L). +, Log 1; ●, Log 2; ∗, Log 3; ○, Log 4.

distance from the board centroid C to the centre of the pith. If boards were cut from a log which had annual rings that surrounded the pith perfectly symmetrically, the (r_L, θ_L) and (r_0, θ_0) coordinates should be exactly the same. The logs for this project were selected to be as symmetrical about the pith as possible, but in nature a log cross-section is never perfectly symmetrical. The under-bark radius of the four quadrants of the discs is shown in Table 2. Figure 11 shows the relationship between the annual ring orientation(θ_0)measured with the overlay method and that measured in the log (θ_L). Though a few boards showed considerable variation an excellent correlation was found between them ($r=+0.977$). Figure 12 shows the relationship between the distance from the pith measured within the log (r_L) and the radius of curvature (r_0) measured with the overlay method. There is much greater variability than in Figure 11, although the correlation is still very high ($r=+0.859$). The differences are not only due to deviations from symmetry within the logs. It is obviously easier to accurately draw a line perpendicular to the annual rings and measure its angle to the board surface than it is to determine differences in curvature between nearly straight

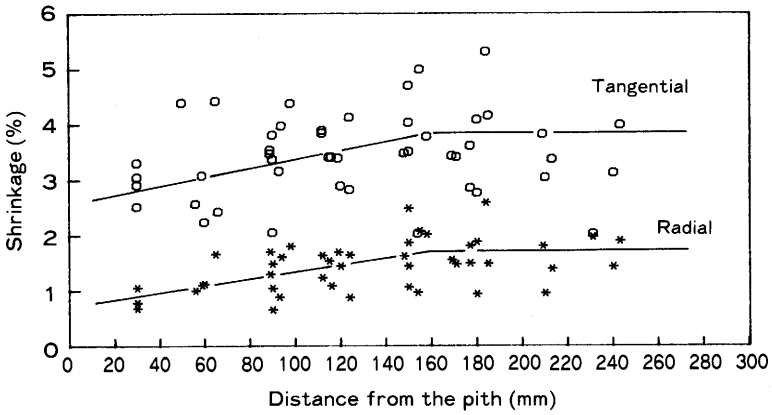

Fig. 13. Radial distribution of tangential and radial shrinkage to 12 %mc.

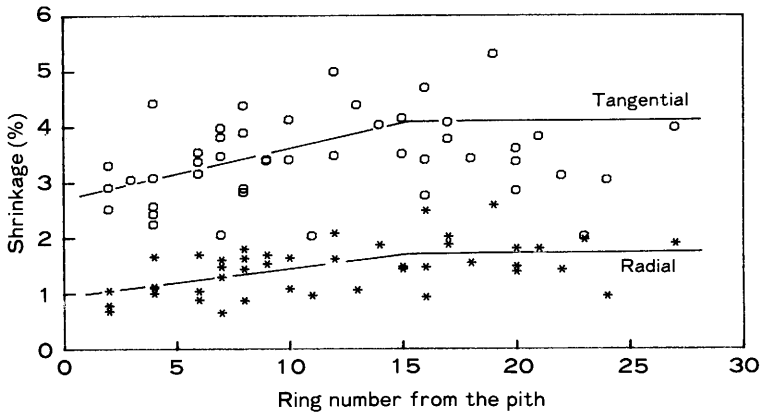

Fig. 14. Radial distribution of tangential and radial shrinkage to 12 %mc.

lines at large r values.

4.3 The variation of shrinkage in the three principal directions with radial position in the log

It was found that the shrinkage coefficients for the four logs at the butt end were very similar, hence the results have been combined into one graph of % shrinkage versus distance from the pith (Fig. 13). Tangential and radial shrinkage increased outwards from the pith to about 150 mm and then became constant. This distance corresponds to about 15 rings from the pith (Fig. 14). There were no apparent differences in tangential and radial shrinkage values between the butt and top ends of the logs and the shrinkage graph equivalent to Figure 13 for the top ends of the logs was very similar. While there was this slight tendency for the transverse shrinkage to decrease in the core region, in practice it would be adequate for most purposes to treat the shrinkage coefficients as constants, 3.8% for tangential shrinkage and 1.3% for radial shrinkage. The shrinkage coefficients were determined at 12% m.c.

The longitudinal shrinkage was so small that the experimental error of $\pm 0.1\%$ is of the same order as many of the values. However, Figure 15 is adequate for showing the trend.

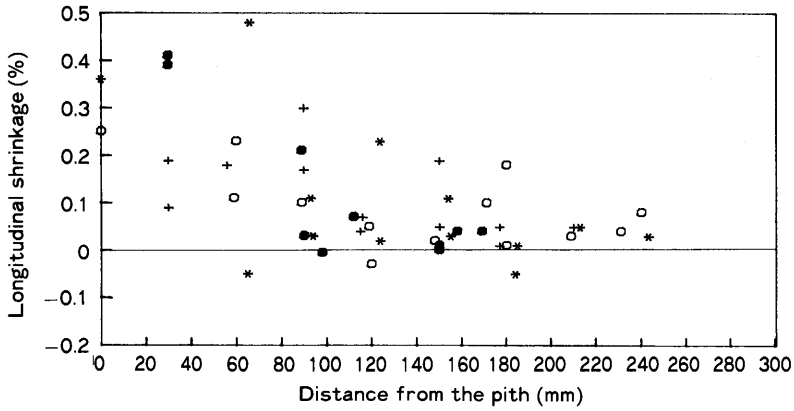

Fig. 15. Radial distribution of longitudinal shrinkage to 12 %mc. +, Log 1; ●, Log 2; ∗, Log 3; ○, Log 4.

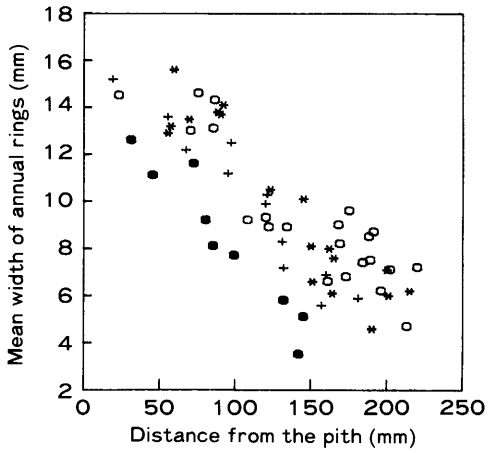

Fig. 16. Relationship between mean width of the annual rings and the distance from the pith. +, Log 1; ●, Log 2; ∗, Log 3; ○, Log 4.

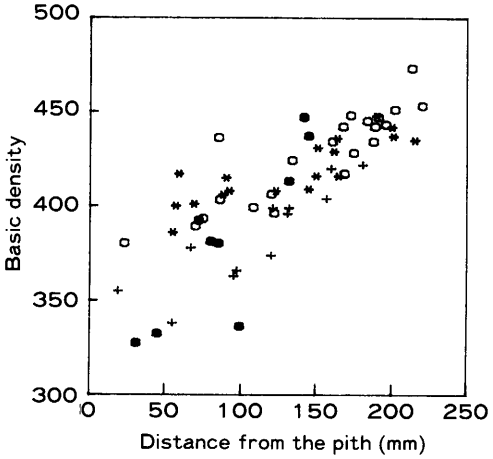

Fig. 17. Radial distribution of basic density. +, Log 1; ●, Log 2; ∗, Log 3; ○, Log 4.

Longitudinal shrinkage is high near the pith and levels off at a distance of about 100 mm from the pith. It will be shown later that this phenomenon affects bow and crook in the core region.

4.4 The variation of ring width and density with distance from the pith

For the four logs the relationship between the distance of the annual rings from the pith and the mean annual ring width for the four logs was determined (Fig. 16). A similar relationship was determined for the density (Fig. 17). In individual logs there was a good negative correlation between r_L and mean annual ring width; the correlation coefficient r for logs 1 to 4 was respectively −0.958, −0.958, −0.931 and −0.891. When data for the four logs were combined the correlation coefficient dropped to −0.817. The correlation between r_L and basic density was poorer than with mean annual ring width (r=0.885, 0.860,

0.849 and 0.875 respectively). When data for the four logs were combined the correlation coefficient dropped to 0.806.

4.5 The direction of warping

(a) Crook

As shown in Table 3, 57% of the boards developed negative crook during or after sawing while still green, while after drying 84% of the boards had positive crook. Of the ten boards with negative crook after drying, four already had negative crook prior to drying, while six had positive crook while green. Except for one board negative crook occurred at large values of r_L and θ_L. Several of the ten boards had cross-grain and knots made a large contribution to the observed crook.

Table 3. Direction of warping

(1) Crook

Direction of crook	Number of boards, green[1]	Average crook, green (mm)	Average crook, dry (mm)[2]	Number of boards after drying			Total number of boards after drying[3]
				+ve	−ve[4]	0	
Positive	24 (39%)	6.3±5.0	16.4±27.5	18	6	0	51 (84%)
Negative	35 (57%)	−6.8±4.0	18.6±20.1	31	4	0	10 (16%)
0	2 (4%)	0	17.0±16.9	2	0	0	0 (0%)
Total/average	61 (100%)	−1.4±7.7	17.7±22.9	51	10	0	61 (100%)

(2) Bow

Direction of bow	Number of boards, green[1]	Average bow, green (mm)	Average bow, dry (mm)[2]	Number of boards after drying			Total number of boards after drying[3]
				+ve	−ve[4]	0	
Positive	18 (30%)	8.6±6.5	19.0±11.3	17	1	0	50 (82%)
Negative	37 (60%)	−7.2±4.4	13.4±18.0	28	9	0	11 (18%)
0	6 (10%)	0	9.1±13.6	5	1	0	0 (0%)
Total/average	61 (100%)	−1.8±8.6	14.9±15.9	50	11	0	61 (100%)

(3) Twist

Direction of twist	Number of boards, green[1]	Average twist, green (mm)	Average twist, dry (mm)[2]	Number of boards after drying			Total number of boards after drying[3]
				+ve	−ve[4]	0	
Positive	32 (52%)	3.6±2.0	4.0±18.6	12	20	0	24 (39%)
Negative	11 (18%)	−3.7±1.5	12.4±31.5	4	6	1	36 (59%)
0	18 (30%)	0	8.3±20.2	8	10	0	1 (2%)
Total/average	61 (100%)	−1.2±3.2	6.8±21.7	24	36	1	61 (100%)

[1] The figures in parenthesis give the % of the total this number of boards represents.

[2] This is the average warp after drying of the boards referred to in the second column (e. g., for the first line it is the crook after drying of the 24 boards which had positive crook while green).

[3] This is the total number of boards that after drying had the direction of warp specified in the first column.

[4] +ve: positive, −ve: negative.

Table 4. Grain direction and direction of twist of the boards

	Number of boards with		
	Positive twist	Negative twist	Zero twist
Positive grain	29* (12, 17, 0)**	10 (4, 5, 1)	16 (8, 8, 0)
Negative grain	2 (0, 2, 0)	1 (0, 1, 0)	2 (0, 2, 0)
Straight grain	1 (0, 1, 0)	0	0
Total	32	11	18

* The numbers outside the parentheses indicate the numbers of green boards in each category.

** The numbers in parenthesis indicate the numbers of the above boards that after drying had positive, negative and zero twist respectively.

Twenty four boards had positive crook before drying. Their average crookwas 6.3±5.0 mm, which increased after drying to 16.4±27.5 mm, an increase of 10.1 mm. In contrast, 35 green boards had negative crook. Their average crook was −6.8±4.0 mm, which increased after drying to 18.6±20.1 mm, an increase of 25.4 mm. In spite of the difference in incremental crook development during drying for the two series of boards, their average crook after drying was very similar. Very apparent is the strong tendency for the boards to develop positive crook on drying, from −1.4±7.7 mm green to 17.7±22.9 mm dry.

(b) Bow

Table 3 shows that 18 boards (30% of the total) developed positive bow during or after sawing while still green. The average bow was 8.6±6.5 mm, which increased after drying to 19.0±11.3 mm, an increase of 10.4 mm. In contrast, 37 green boards (60%) had negative bow, which increased on drying from −7.2±4.4 mm to 13.4±18.0 mm, an increase of 20.6 mm. After drying 82% of the boards had positive bow. The strong tendency to develop positive bow on drying is also indicated by the change in average bow from −1.8±8.6 mm to 14.9±15.9 mm on drying.

(c) Twist

As shown in Table 3, thirty percent of the green boards had no twist, half the green boards had positive twist and 18% had negative twist. After drying 59% had developed negative twist. Nevertheless the average twist increased from −1.2±3.2 mm to 6.8±21.7 mm.

The relationship between spiral grain direction and the direction of twist is investigated in Table 4. The spiral grain was measured on the specimens cut from the boards (Fig. 2). Of the 32 green boards with positive twist 29 had a positive grain direction while only 2 had negative grain direction. Of the 11 green boards with negative twist 10 also had positive grain, so the off-the-saw twist does not seem to be related to spiral gain direction. According to Table 4 there does not seem to be a strong relation between grain direction and twist after drying. This is contradicted by subsequent sections of this report. The reason for this contradiction is probably that boards can never be sawn exactly parallel to the tree axis, so that the grain angle measurements on board offcuts (cf. Fig. 2) are not very accurate. Taking spiral grain measurements on diametrically opposite sides of a diametral strip and averaging prevents the above error.

4.6 Radial distribution of spiral grain deviation and its effect on the twist of boards

Figures 18 to 21 show graphs of spiral grain deviation in each log versus distance from

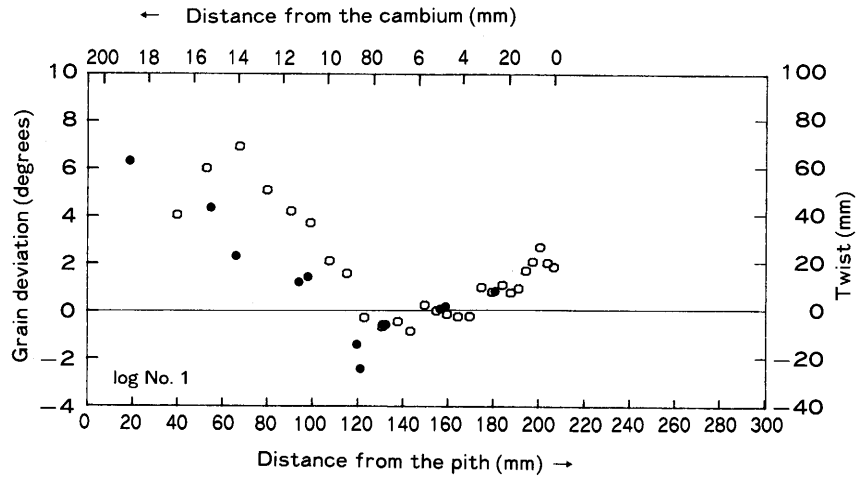

Fig. 18. Radial distribution of grain deviation and twist after drying for log No. 1. An open circle represents the grain deviation, while a closed circle represents the twist value obtained for a board whose centroid was located at the distance from the pith shown on the graph. The grain deviation is the average of two values obtained on opposite sides of a diametral strip and is also averaged over the top and butt ends of the log.

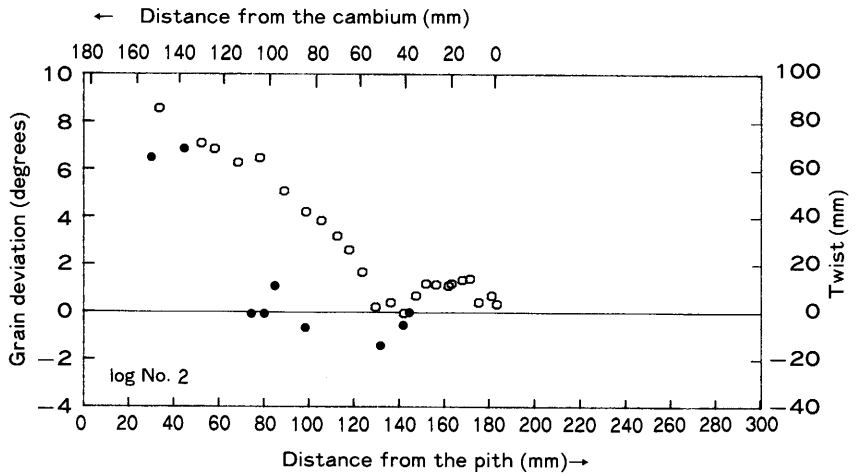

Fig. 19. Radial distribution of grain deviation and twist after drying for log No. 2. Open circles represent grain deviation, while closed circles indicate twist.

the pith (r_L). On the same graphs are plotted twist versus distance from the pith for the boards cut from that particular log. Open circles above the zero line represent positive or S-type grain deviation, while solid black circles above the zero line represent positive or S-type twist. If log no. 2 is disregarded, the boards from regions with a grain deviation above +3 degrees showed S-type twist after drying, whereas boards from regions with a grain deviation of less than 3 degrees showed Z-type twist. In log 2 two boards with a grain deviation in excess of six degrees showed S-type (+ve) twist, while two other boards with a grain deviation of 6 degrees showed negative twist. The latter are considered anomalous.

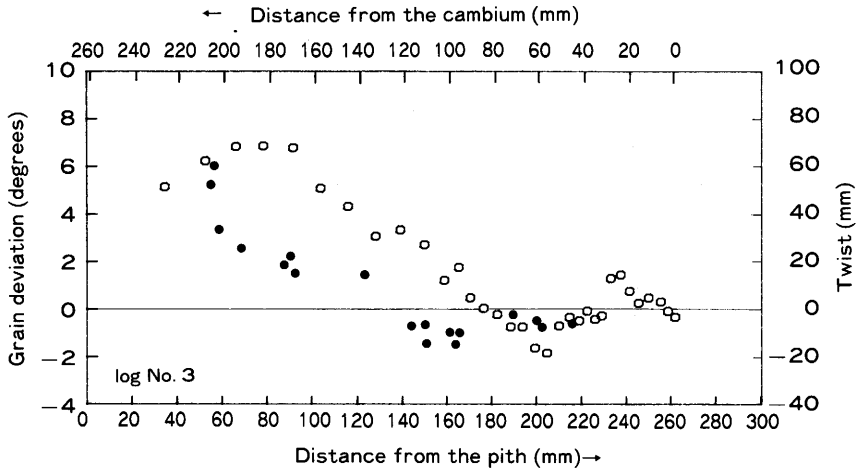

Fig. 20. Radial distribution of grain deviation and twist after drying for log No. 3. Open circles represent grain deviation, while closed circles represent twist.

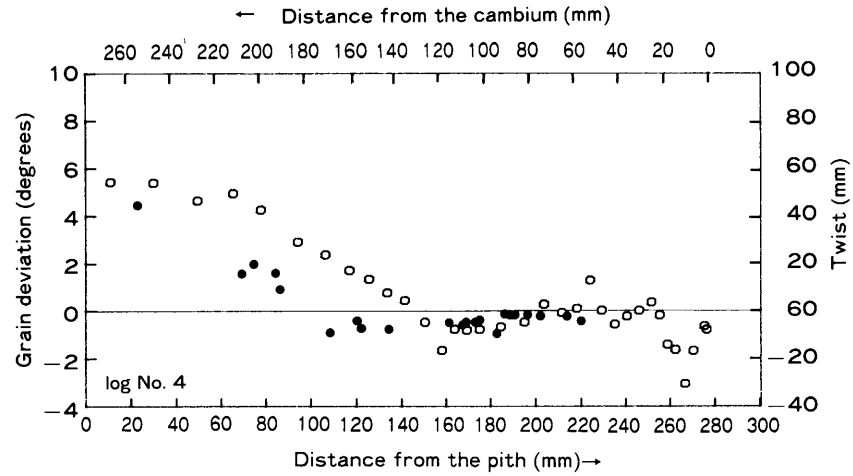

Fig. 21. Radial distribution of grain deviation and twist after drying for log No. 4. Open circles represent grain deviation, while closed circles represent twist.

One, a flat-sawn board, had large bow and a kink caused by local cross-grain, while the other which was nearly quartersawn had its centroid on the outer corewood boundary and had anomalously large crook. These factors are believed to have contributed to the negative (Z-type) twist.

The grain deviation in the logs changed from S- to Z-type at about 150 mm (120 to 180 mm)from the pith. This corresponds to about 13 rings (10 to 15 rings) from the pith. At a distance beyond 150 mm from the pith the grain deviation became small. Almost all boards sawn from the regions where the deviation was small showed a small amount of Z-twist.

4.7 Relationships between twist, crook, bow and various other parameters

(a) Mean width of annual rings

As shown in Figure 22, boards containing pith twisted much more severely than

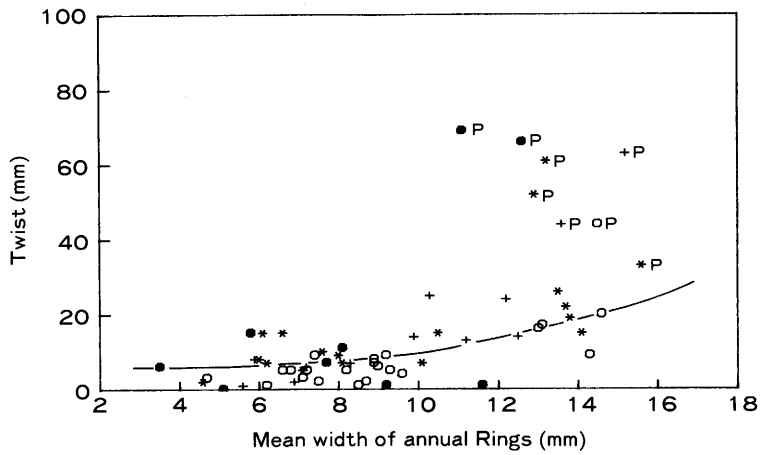

Fig. 22. Relationship between twist and mean width of the annual rings. +, Log 1; ●, Log 2; *, Log 3; ○, Log 4. P, boards with pith.

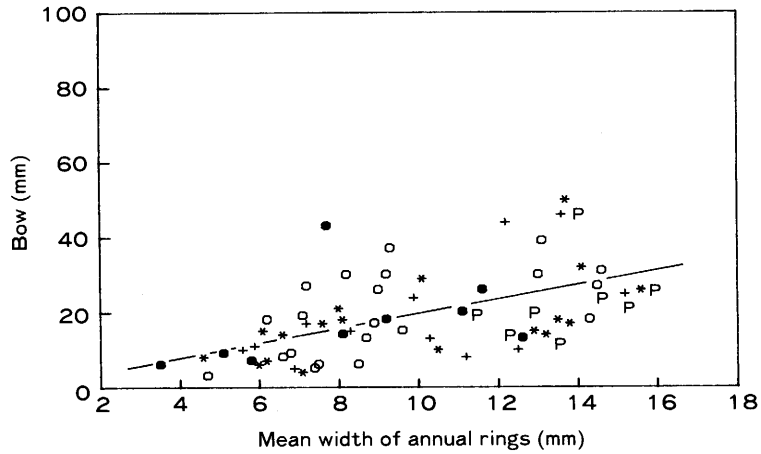

Fig. 23. Relationship between bow and mean width of the annual rings. +, Log 1; ●, Log 2; *, Log 3; ○, Log 4. P, boards with pith.

boards without pith. When the 8 boards with pith were excluded, a tendency was observed for the twist to increase with increasing mean width of the annual rings (r=0.652). In individual logs a good correlation was found between them (r=0.799, 0.543, 0.796 and 0.821 resp. for boards from logs 1 to 4).

It would however be completely wrong to draw the conclusion that a board from a tree with large growth rings will necessarily have a lot of twist. Twist is related to spiral grain. Annual rings are widest near the pith (Fig. 16) and the region near the pith also has the largest spiral grain (Figs. 18 to 21). Hence the good correlations between twist and ring width are very unlikely to mean that boards from a tree with large annual rings will show more twist than boards from a tree of the same diameter with narrow annual rings.

In strong contrast with twist, the pith had no apparent influence on bow and crook. Consequently it was not necessary to consider boards with and without pith separately to examine the relationship between bow, crook and ring width.

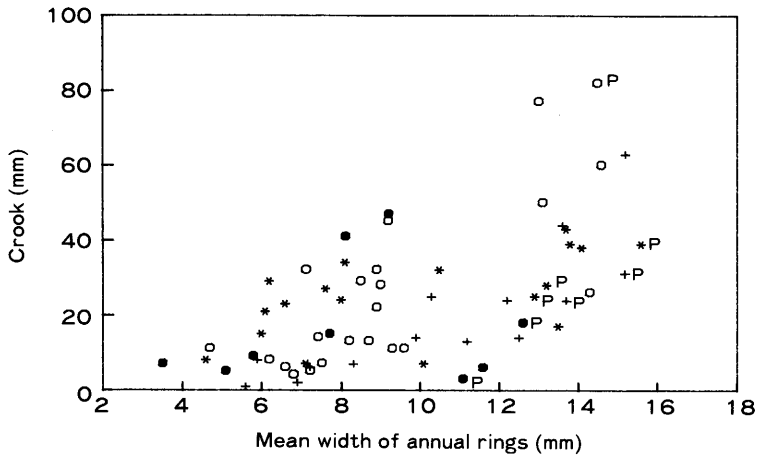

Fig. 24. Relationship between crook and mean width of the annual rings. +, Log 1; ●, Log 2; ∗, Log 3; ○, Log 4; P, boards with pith.

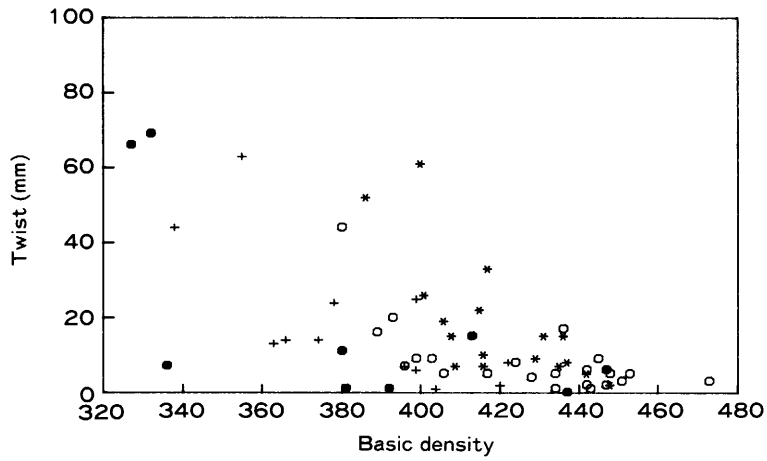

Fig. 25. Relationship between twist and basic density. +, Log 1; ●, Log 2; ∗, Log 3; ○, Log 4.

Bow had a tendency to increase with increasing annual ring width (Fig. 23), but there was only a poor correlation between them ($r=0.547$). Even for boards from the same log the correlations were very poor, ranging from a minimum of 0.380 to a maximum of 0.593.

Crook also had a tendency to increase with increasing annual ring width (Fig. 24), but the correlation was poor ($r=0.591$). The correlations between bow and crook versus annual ring width can be explained in similar terms as the correlation between twist and ring width. Ring witdh is greatest near the pith. The region around the pith consists of corewood, which causes differential longitudinal shrinkage which usually causes severe bow and crook. This will be discussed further in secton 4.9.

(b) Basic density (ρ)

Twist has a slight tendency to decrease with increasing basic density (Fig. 25), but the correlaton is poor ($r=-0.627$ for a linear analysis, $r=-0.653$ for a quadratic). The correlation was slightly better for individual logs, the correlation coefficients (r) for logs 1 to 4 being respectively 0.750, 0.799, 0.757, and 0.764. Basic density was not correlated with

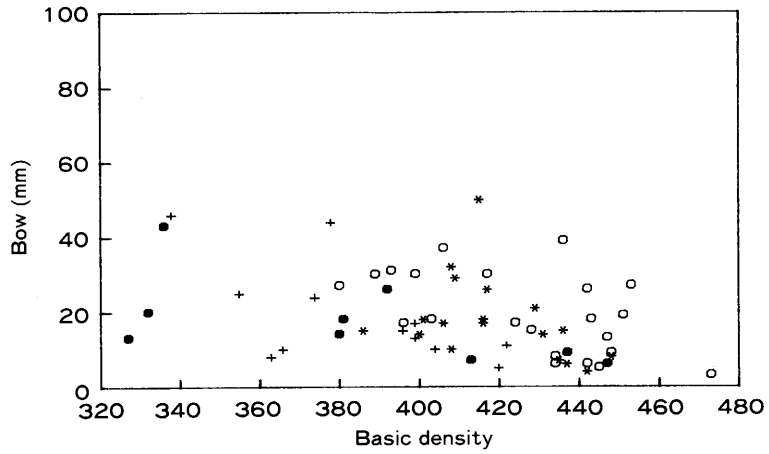

Fig. 26. Relationship between bow and basic density. +, Log 1; ●, Log 2; ∗, Log 3; ○, Log 4.

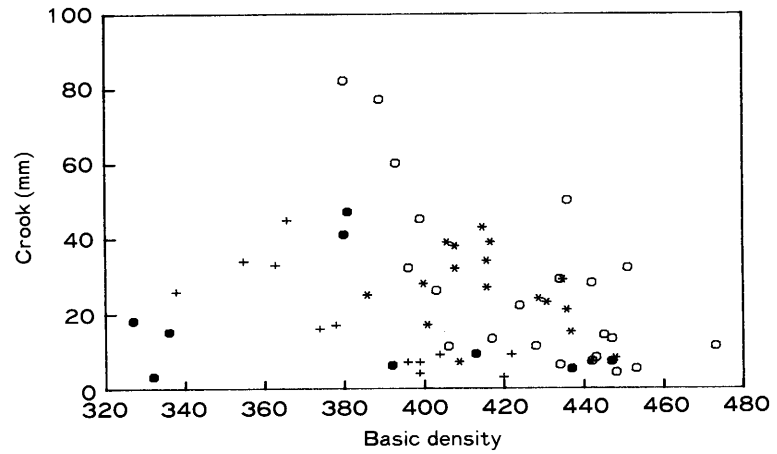

Fig. 27. Relationship between crook and basic density. +, Log 1; ●, Log 2; ∗, Log 3; ○, Log 4.

bow and crook (Figs. 26 and 27), but in individual logs bow and crook had a tendency to decrease with increasing basic density. Again, it should be borne in mind that basic density increases with distance from the pith for all four logs.

(c) Grain deviation (ϕ)

All boards that contained pith twisted very severely compared with those without pith. Figure 28 shows that when the boards with pith were excluded, twist had a tendency to increase with increasing ϕ, although the correlation was poor ($r=0.560$).

The grain deviation showed no correlation with bow (Fig. 29) or crook (Fig. 30) overall or even within individual logs.

Figure 31 shows the relationship between twist and grain deviation obtained from the diametral spiral grain strips (cf. section 2.4b). These data were already presented in a different way in section 4.6 and Figures 18 to 21. The twist shows a tendency to increase with increasing grain deviation in both the positive and negative directions. Twist increases according to a quadratic equation in regions with a grain deviation of more than

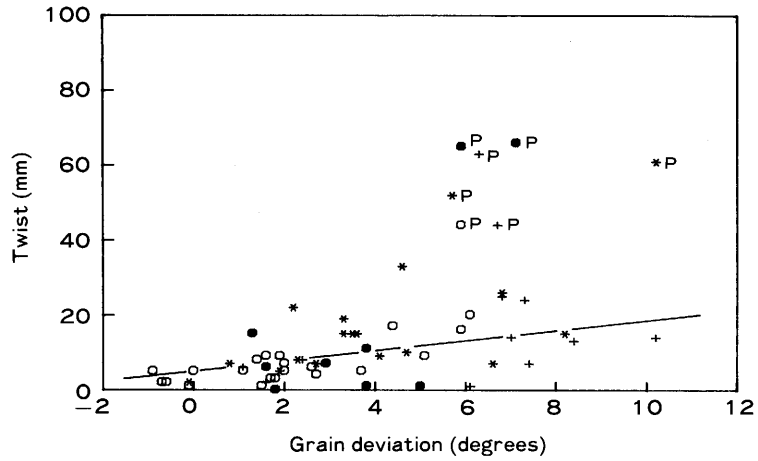

Fig. 28. Relationship between twist and grain deviation (determined on 100 mm long spiral grain specimens). +, Log 1; ●, Log 2; ∗, Log 3; ○, Log 4; P, boards with pith.

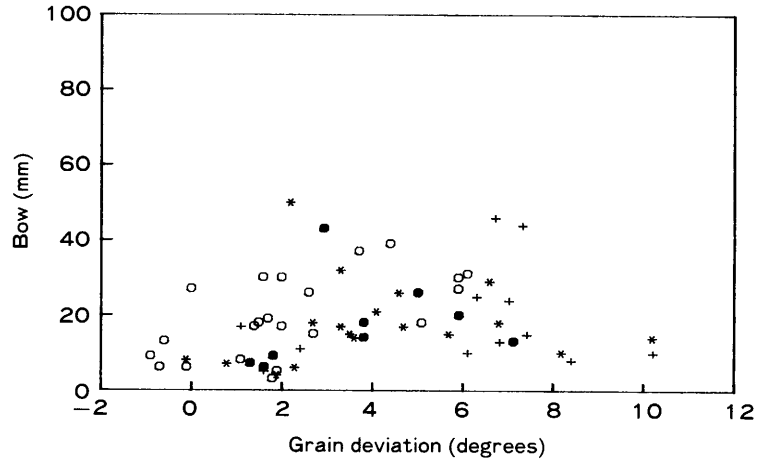

Fig. 29. Relationship between bow and grain deviation. +, Log 1; ●, Log 2; ∗, Log 3; ○, Log 4.

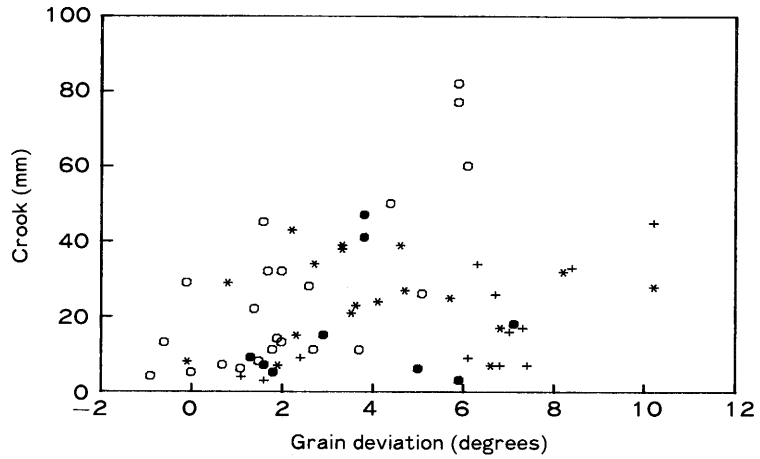

Fig. 30. Relationship between crook and grain deviation. +, Log 1; ●, Log 2; ∗, Log 3; ○, Log 4.

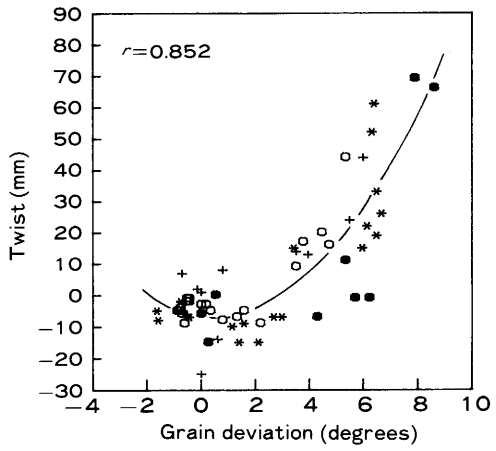

Fig. 31. Relationship between twist and grain deviation from figures 18 to 21. +, Log 1; ●, Log 2; ∗, Log 3; ○, Log 4.

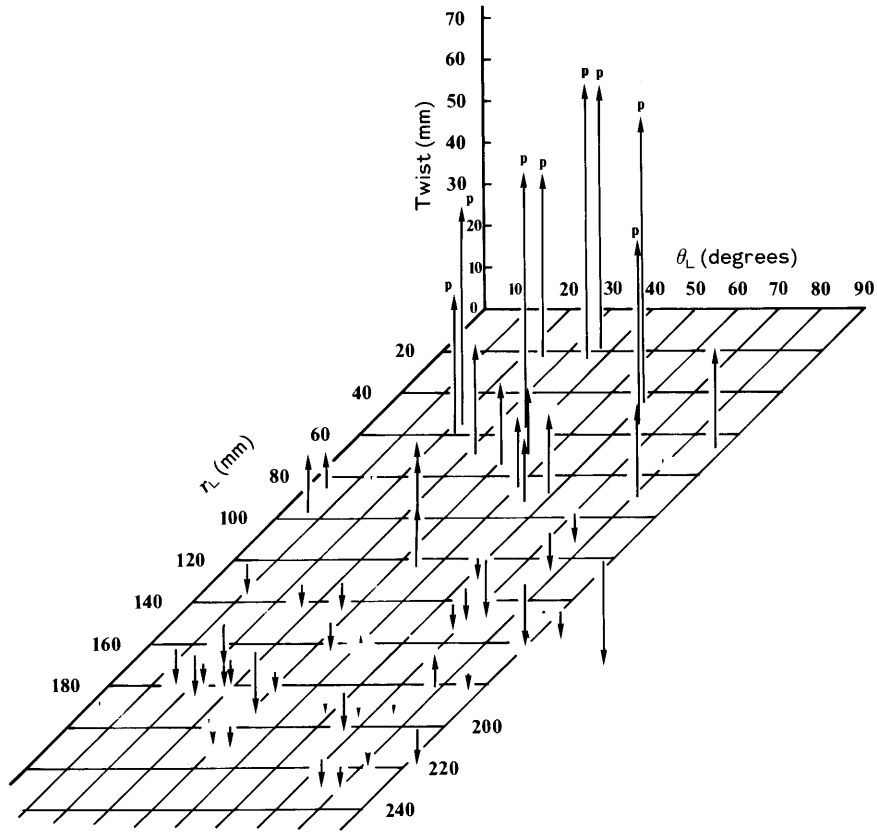

Fig. 32. Relationship between twist and the r_L and θ_L coordinates. r_L; average distance from the centroid of the two end cross-sections of each board to the pith, as measured in the log assemble. θ_L: average annual ring angle co-ordinate for the two end cross-sections of each board, as measured in the log assemble. P: boards with pith. The position coordinates of each board are represented by the base of each arrow, while the length represents the magnitude in the positive or negative direction.

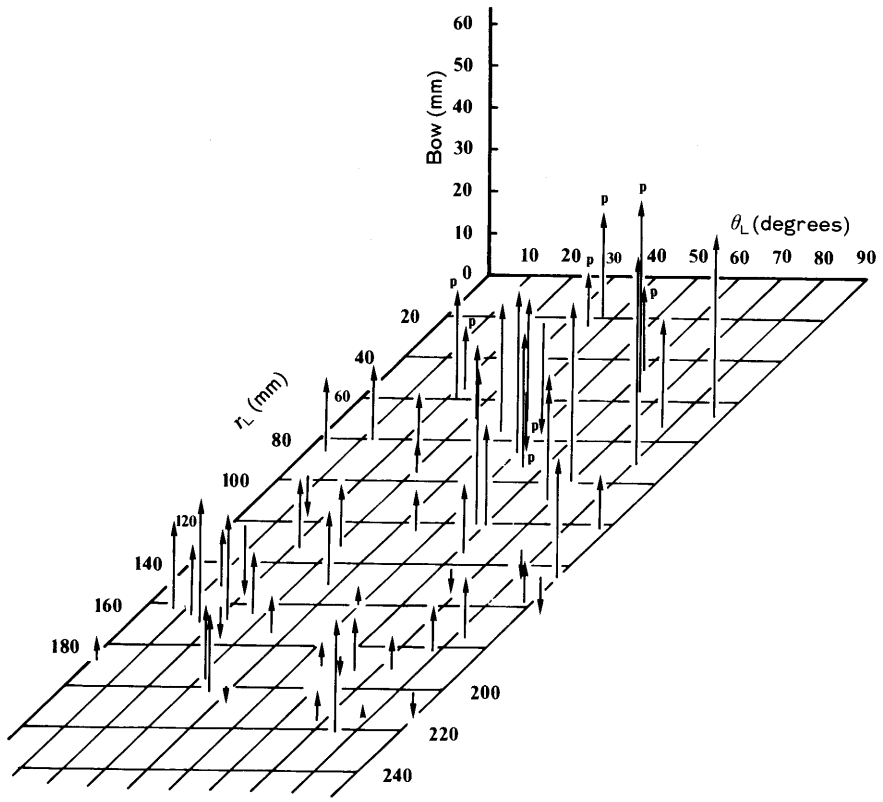

Fig. 33. Relationship between bow and the r_L and θ_L coordinates. r_L: average distance from the centroid of the two end cross-sections of each board to the pith, as measured in the log assemble. θ_L: average annual ring angle co-ordinate for the two end cross-sections of each board, as measured in the log assemble. P: boards with pith. The position coordinates of each board are represented by the base of each arrow, while the length represents the magnitude in the positive or negative direction.

four degrees with a correlation coefficient of 0.85.

4.8 The relationship between twist, bow and crook and the board coordinates (r, θ)

The relationship between twist, bow and crook and the board coordinates r_L and θ_L are shown respectively in Figures 32 to 34. Here r_L is the average distance from the centroid of the two board endfaces to the pith and θ_L is the average angle, both coordinates being measured in the reassembled log (Fig. 10). Positive bow, crook and twist are represented by upward arrows in Figures 32 to 43, while negative values are indicated by arrows pointing downwards. The board coordinates are represented by the base of each arrow. Boards that contained pith twisted severely. Twist had a tendency to decrease with increasing r_L irrespective of θ_L. Almost all boards from the outer wood showed negative (Z-type) twist, irrespective of θ_L.

The presence of pith had no apparent influence on bow and crook (Figs. 33 and 34). Bow showed a tendency to decrease with decreasing θ_L in the corewood region, while in the outerwood region bow tended to decrease with increasing θ_L. Only a few boards developed negative bow, which was never large. Negative bow occurred mainly at large values of r_L.

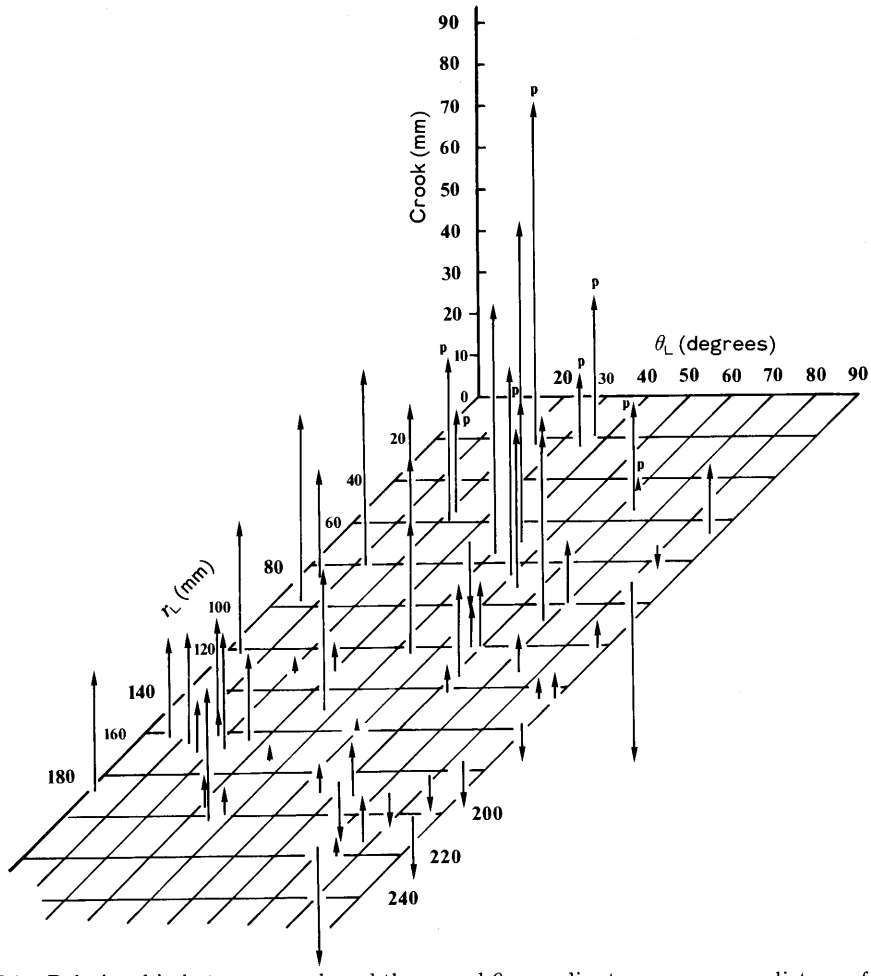

Fig. 34. Relationship between crook and the r_L and θ_L coordinates. r_L: average distance from the centroid of the two end cross-sections of each board to the pith, as measured in the log assemble. θ_L: average annual ring angle co-ordinate for the two end cross-sections of each board, as measured in the log assemble. P: boards with pith. The position coordinates of each board are represented by the base of each arrow, while the length represents the magnitude in the positive or negative direction.

Crook showed a tendency to decrease with increasing r_L and θ_L. Negative crook occurred at large θ_L values, irrespective of r_L. Figures 35 to 37 show the relationships between twist, crook and bow respectively and the coordinates (r_0, θ_0). Here r_0 and θ_0 are the average (r_0, θ_0) coordinates of the two board endfaces measured with the overlay method (refer p. 5). In general the variation of twist, crook and bow with r_0 and θ_0 is similar to the variation with r_L and θ_L, as would be expected because of the high correlation between θ_0 and θ_L and r_0 and r_L (Figs. 11 and 12 respectively).

The true twist (twist*) of a board is the twist value obtained by subtracting the twist of the green board from the twist in the dry board. Crook* and bow* are similarly defined. Values of twist*, bow* and crook* are plotted as a function of r_L and θ_L in Figures 38 to 40. The general relationship between twist* and crook* and the r_L and θ_L coordinates was

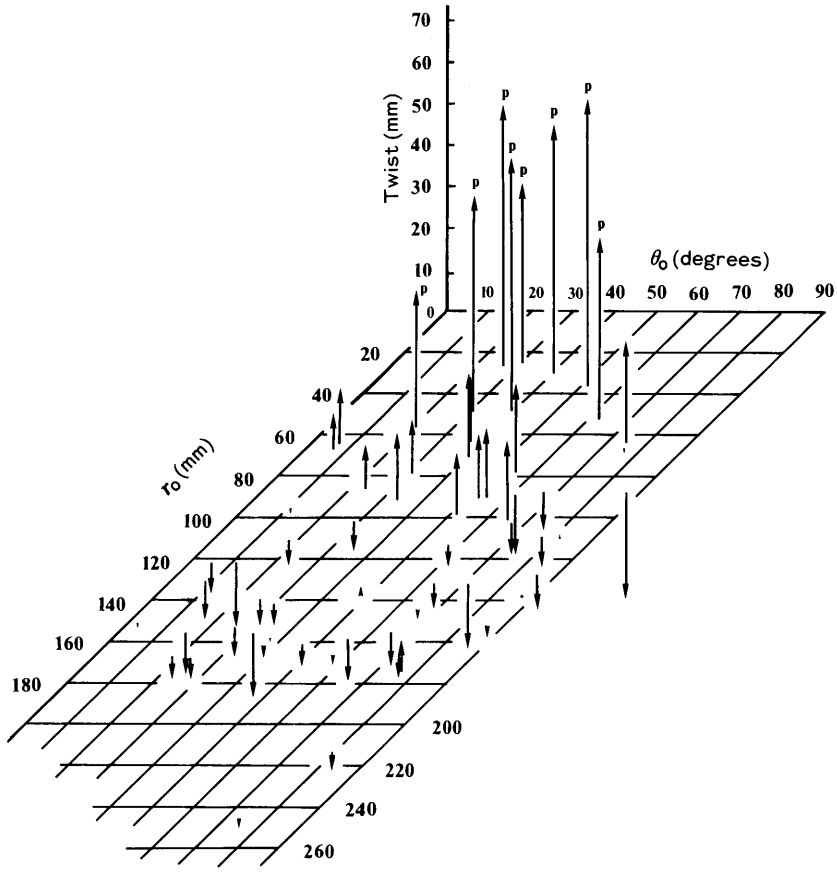

Fig. 35. Relationship between twist and the r_0 and θ_0 coordinates. r_0: average distance from the centroid of the two end cross-sections of each board to the pith, as measured by the overlay method. θ_0: average annual ring angle co-ordinate for the two end cross-sections of each board, as measured by the overlay method. P: boards with pith.

similar to those shown in Figures 32 and 34. However, the relationships for bow were now not as clear.

Figures 41 to 43 show the relationship between twist, crook and bow and the (r_8, θ_8) coordinates. Here r_8 and θ_8 are the average r_0 and θ_0 coordinates obtained by the overlay method for eight reference specimens cut at 1 m intervals along the boards. The general variation of twist, crook and bow with the r_8 and θ_8 coordinates was similar to that for the r_L and θ_L coordinates in Figures 32 to 34.

4.9 Explanation of the properties of the three dimensional graphs in terms of corewood properties

The interior region of a log known as corewood has relatively high longitudinal shrinkage and large spiral grain compared with the mature wood (COWN and MCCONCHIE, 1983a and b). In radiata pine the corewood region extends about 10 annual rings, corresponding to a radius of about 100 to 150 mm (COWN D. J., pers. com.). In section 4.3 and Figures 13 to 15 it was shown that for our logs the corewood boundary also occurred at a

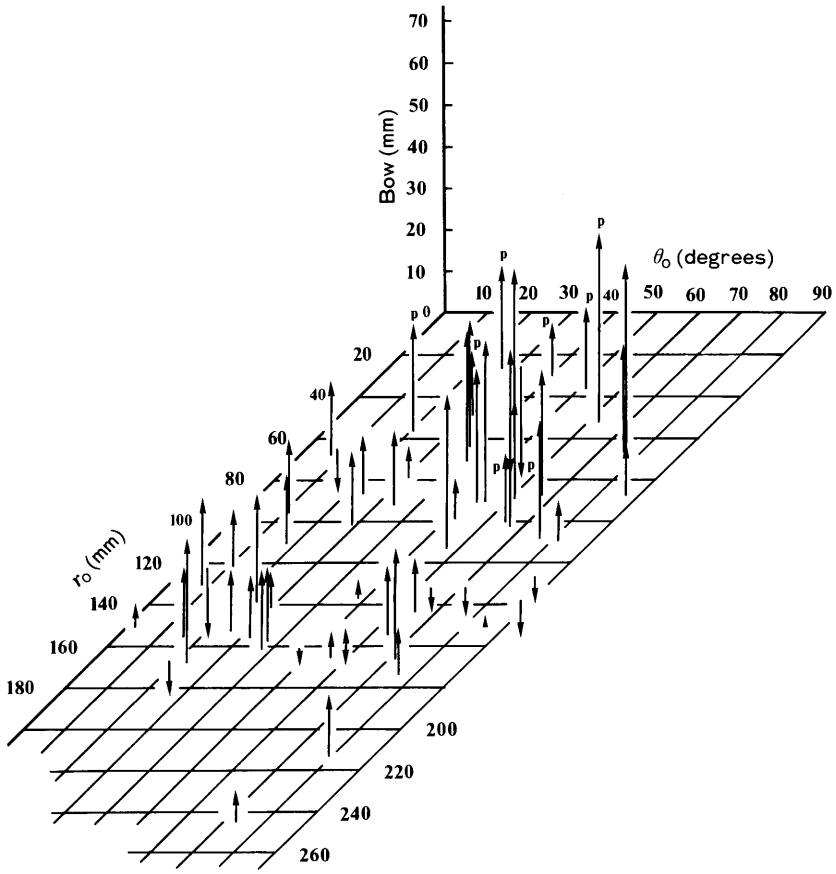

Fig. 36. Relationship between bow and the r_0 and θ_0 coordinates. r_0: average distance from the centroid of the two end cross-sections of each board to the pith, as measured by the overlay method. θ_0: average annual ring angle co-ordinate for the two end cross-sections of each board, as measured by the overlay method. P: boards with pith.

distance of 100–150 mm from the pith. This corresponds to a core consisting of 10 to 15 annual rings. According to Figures 18 to 21 wood with a large grain angle extended for a radial distance of about 150 mm. Consequently it can be safely assumed that the corewood is a cylinder with a radius of 150 mm. The effect of corewood upon bow and crook will be discussed by reference to Figure 44. The quartersawn board A has a centroid that lies on the outer boundary of the corewood. The right hand side of the board lies in the mature wood, while the left hand side lies in the corewood region, so that the left hand side shrinks more along the board's length than the right hand side. The resulting stresses bend the board like a bimetallic strip. The differential shrinkage causes severe crook to develop in board A with the concave side towards the leading edge (positive crook). As board A is completely symmetrical with respect to the x-axis, there is little tendency for this board to develop bow. Board B on the other hand is symmetrical with respect to the y-axis so that differential shrinkage should not introduce crook. However, differential shrinkage should cause severe bow in this case. For boards like C with intermediate ring orientation differential shrinkage should cause both bow and crook, with the concave directions

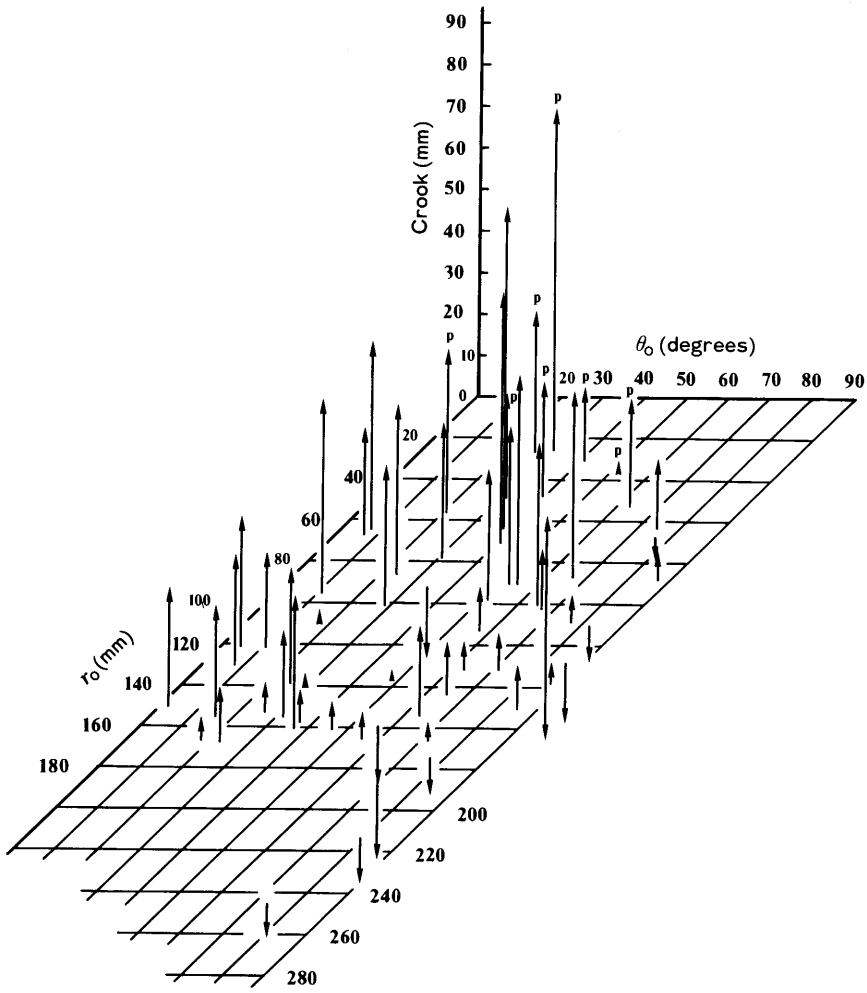

Fig. 37. Relationship between crook and the r_0 and θ_0 coordinates. r_0: average distance from the centroid of the two end cross-sections of each board to the pith, as measured by the overlay method. θ_0: average annual ring angle co-ordinate for the two end cross-sections of each board, as measured by the overlay method. P: boards with pith.

towards the leading edge (i.e., positive bow and crook). Boards like D lying completely in the mature wood will experience little differential shrinkage so that these boards will develop little bow and crook.

The simple model we have discussed above in relation to Figure 44 effectively treats the corewood as uniform and would predict that maximum bow and crook would occur when the centroid lies on the corewood boundary. In reality the longitudinal shrinkage in the corewood increases rapidly towards the pith and consequently bow and crook should increase rapidly as r_L decreases.

The above predictions are confirmed by Figures 34, 37, 40 and 43 that show that crook is small at large values of r, and increases when the centroid approaches the corewood boundary. Within the core crook is large in the positive direction. As predicted, crook

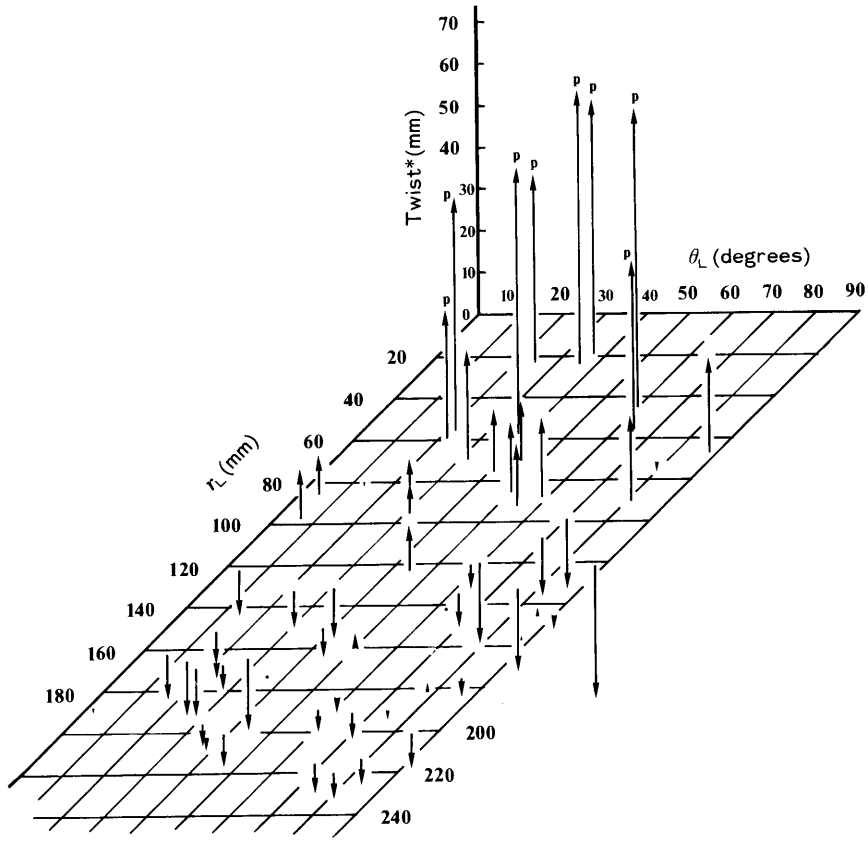

Fig. 38. Relationship between twist* and the r_L and θ_L coordinates. r_L: average distance from the centroid of the two end cross-sections of each board to the pith, as measured in the log assemble. θ_L: average annual ring angle co-ordinate for the two end cross-sections of each board, as measured in the log assemble. P: boards with pith.

reaches a maximum when $\theta=0°$ (quartersawn) and a minimum when $\theta=90°$ (flat-sawn).

The predictions for bow are not satisfied quite as well as those for crook. Figures 33, 36 and 39 show the predicted increase of positive bow when the corewood region is entered, but there is not as clear a minimum at $\theta=0°$ or maximum at $\theta=90°$ as this simple model would indicate.

Conclusion

The aim of this paper was to record the details of the experiment, to record the data obtained, and to analyse them as far as possible. The analysis presented us with severe problems. One major problem was that many of the parameters were found to be interrelated, for instance density, ring width, spiral grain and longitudinal shrinkage all increase or decrease with radial position in the log. If this had not been realised it might for instance have been erroneously concluded that boards from trees with wide annual rings would all experience severe twist on drying (section 4.7(a)).

It was shown that the shape of the three dimensional figures of crook and bow (Figs. 33 and 34) can be explained in terms of differential longitudinal shrinkage between corewood

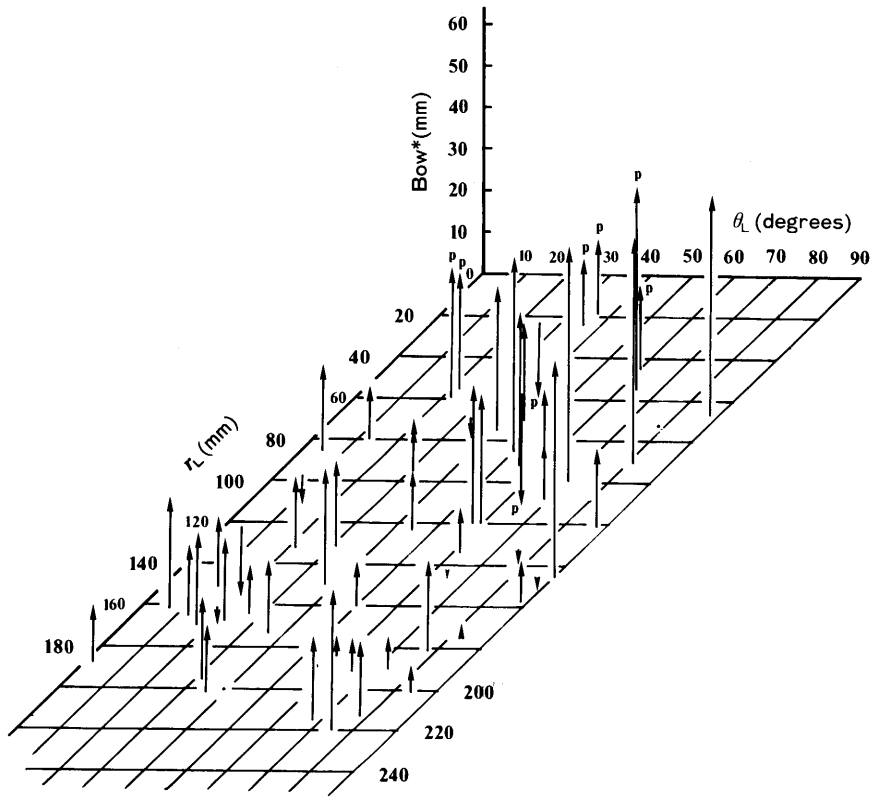

Fig. 39. Relationship between bow* and the r_L and θ_L coordinates. r_L: average distance from the centroid of the two end cross-sections of each board to the pith, as measured in the log assemble. θ_L: average annual ring angle co-ordinate for the two end cross-sections of each board, as measured in the log assemble. P: boards with pith.

and mature wood, and that crook reached a maximum at $\theta=0°$ and a minimum at 90°. If we had sought to analyse crook in terms of the radial parameter only, i.e., if we had reduced the three dimensional graphs to two dimensions, thereby omitting either the effect of θ or of r, these two dimensional graphs would have been quite meaningless. In other words, it follows that it is essential that twist, bow and crook should be analysed in terms of all variables at once. Unfortunately, the total number of boards available for analysis is only 61, as measurements on a greater number would have required an astronomical number of man hours. In addition the degrade of each board is affected to a greater or lesser extent by the presence of knots in different (but known) orientations and of different (known) sizes. For these reasons statistical multi-variant analysis is of no value, and this method of approach looks hopeless.

The best alternative approach that can be taken is to develop a mathematical theory against which the experimental data can be tested. This approach was found to be successful by Booker, Ward and Williams (to be published) for drying degrade in two dimensions (i.e., cupping and diamonding). The new model will be based on the two following assumptions:

(i) twist is caused primarily by spiral grain,

(ii) bow and crook are primarily caused by longitudinal shrinkage differences

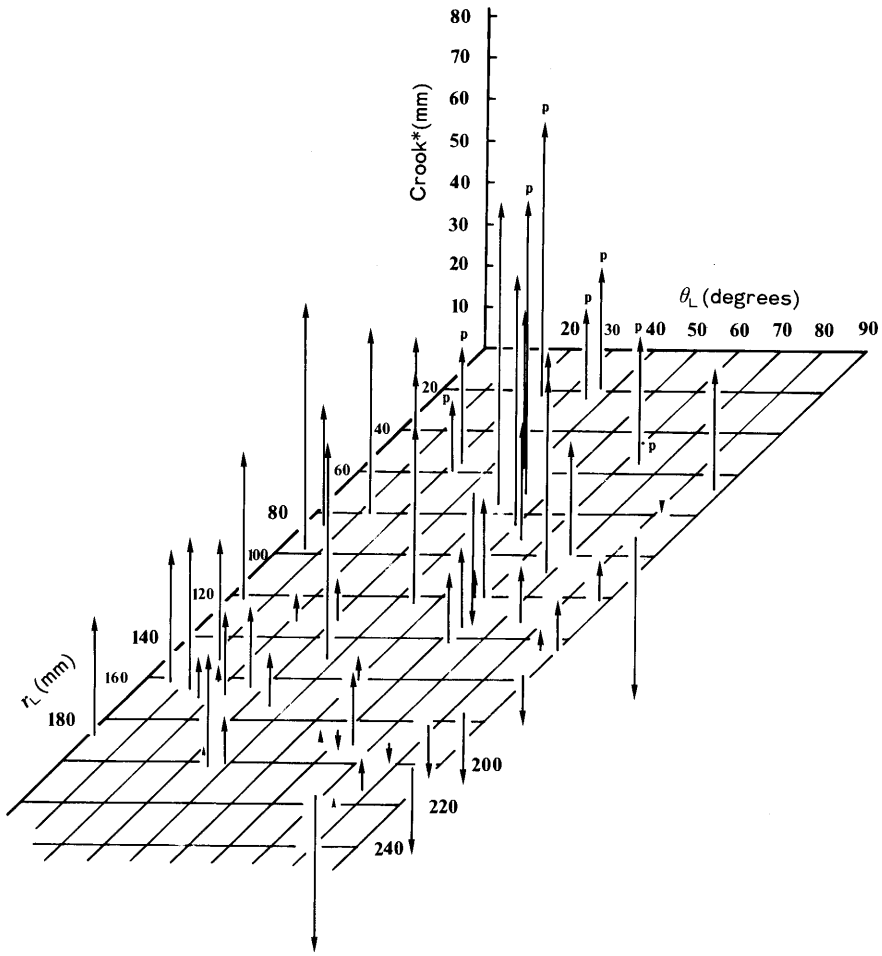

Fig. 40. Relationship between crook* and the r_L and θ_L coordinates. r_L: average distance from the centroid of the two end cross-sections of each board to the pith, as measured in the log assemble. θ_L: average annual ring angle co-ordinate for the two end cross-sections of each board, as measured in the log assemble. P: boards with pith.

between corewood and mature wood.

Preliminary developments indicate that spiral grain not only affects twist, but in addition makes a contribution to bow and crook. The development of this theory and its comparison with the experimental results will be the subject of a subsequent paper.

Acknowledgements

The authors wish to acknowledge the help received in sawing and drying the timber from Mr. J. Maindonald, and Mr. Tom O'Toole from the Timber Industry Training Centre and technical assistance in the measurements from Mr. T. Patmore.

The authors are grateful to Mr. N. Ward and Mr. A. Haslett for selecting the logs and assisting with the log measurements and sawing.

The work was carried out in the Wood Drying Section of the Wood Technology Division, Forest Research Institute, Rotorua, New Zealand.

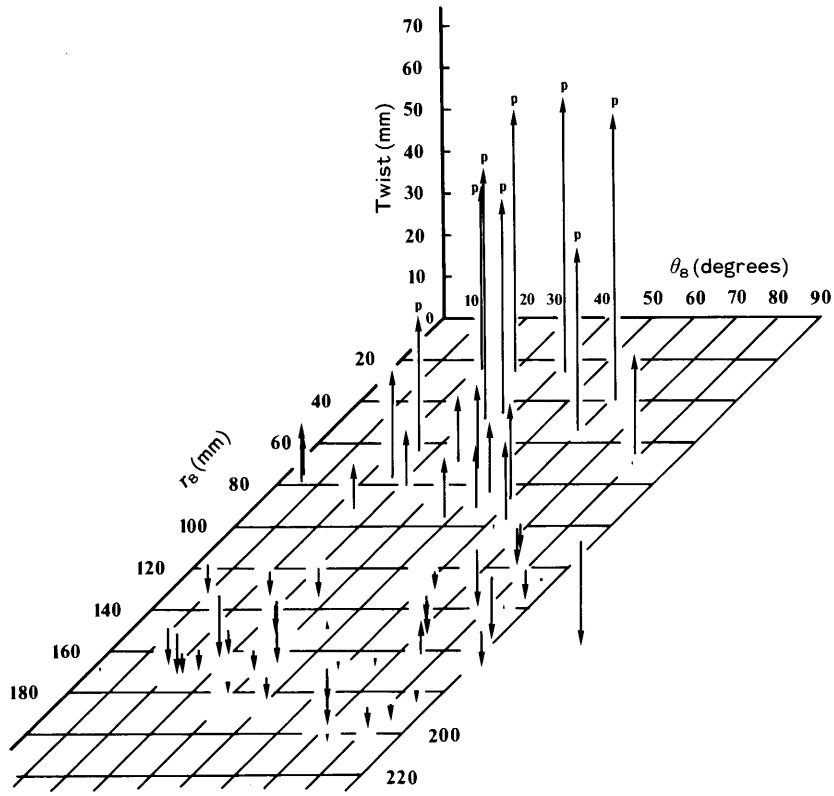

Fig. 41. Relationship between twist and the r_8 and θ_8 coordinates. r_8: average distance from the centroid of the eight cross-sections of each board, as measured by the overlay method. θ_8: average annual ring angle co-ordinate for the eight cross-sections of each board, as measured by the overlay method. P: boards with pith.

Dr. Mishiro gratefully acknowledges receiving a Senior Research Fellowship, awarded by the National Research Advisory Council, during his stay in New Zealand.

Summary

The bow, crook and twist that developed during the unrestrained drying of 61 radiata pine boards were carefully measured. The boards were sawn from four carefully selected logs and the position of each board in the log was accurately specified. The shrinkage coefficients, spiral grain and several other parameters were measured for each log as a function of radial position. The position, size and associated grain deviation of all knots in each board were carefully recorded.

A novel method has been developed to analyse bow, crook and twist. The concept of a leading edge has been introduced. The leading edge is the edge of a board closest to the pith while the board was still part of the log. Bow, crook and twist were measured with respect to the surfaces that contained the leading edge. Positive and negative bow, crook and twist have been carefully defined.

A strong tendency has been found for boards to develop positive crook and positive bow during drying. While the average twist also became more positive during drying, only

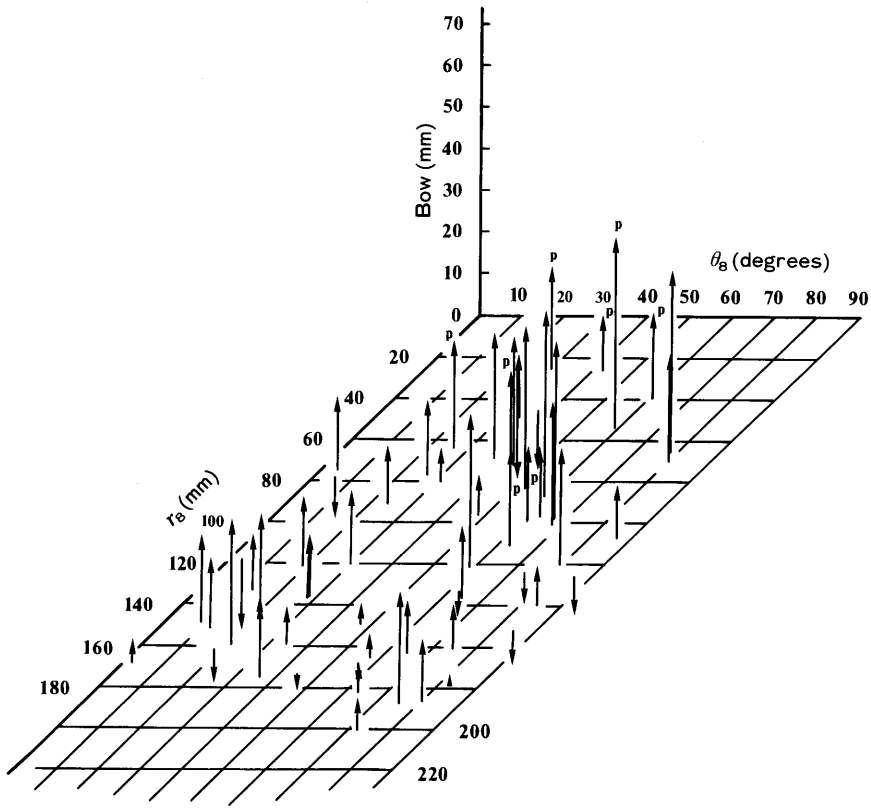

Fig. 42. Relationship between bow and the r_8 and θ_8 coordinates. r_8: average distance from the centroid of the eight cross-sections of each board, as measured by the overlay method. θ_8: average annual ring angle co-ordinate for the eight cross-sections of each board, as measured by the overlay method. P: boards with pith.

about half the boards developed positive twist. Twist was found to be strongly related to spiral grain.

The data were analysed in terms of two board coordinates r and θ where r is the distance of the centroid of the board's cross-section from the pith and θ is a parameter indicating the orientation of the annual rings, where θ ranges from 0 degrees for quartersawn to 90 degrees for flatsawn. The shape of the three dimensional graphs obtained by plotting crook and bow versus r and θ can be explained in terms of differences in longitudinal shrinkage between corewood and mature wood. Crook had a minimum value at a θ value of 90° for all values of r.

Bow, crook and twist were analysed in terms of single parameters such as density, ring width, and distance from the pith. It was found that analysis in terms of single parameters is at best inadequate, while in the worst case it can lead to erroneous conclusions. Multi-variant analysis would be desirable, but as many of the variables are interdependent 61 boards form too small a sample. Yet to study a greater number would be an impossible task. The recommended alternative is the development of a mathematical model against which the experimental data can be tested.

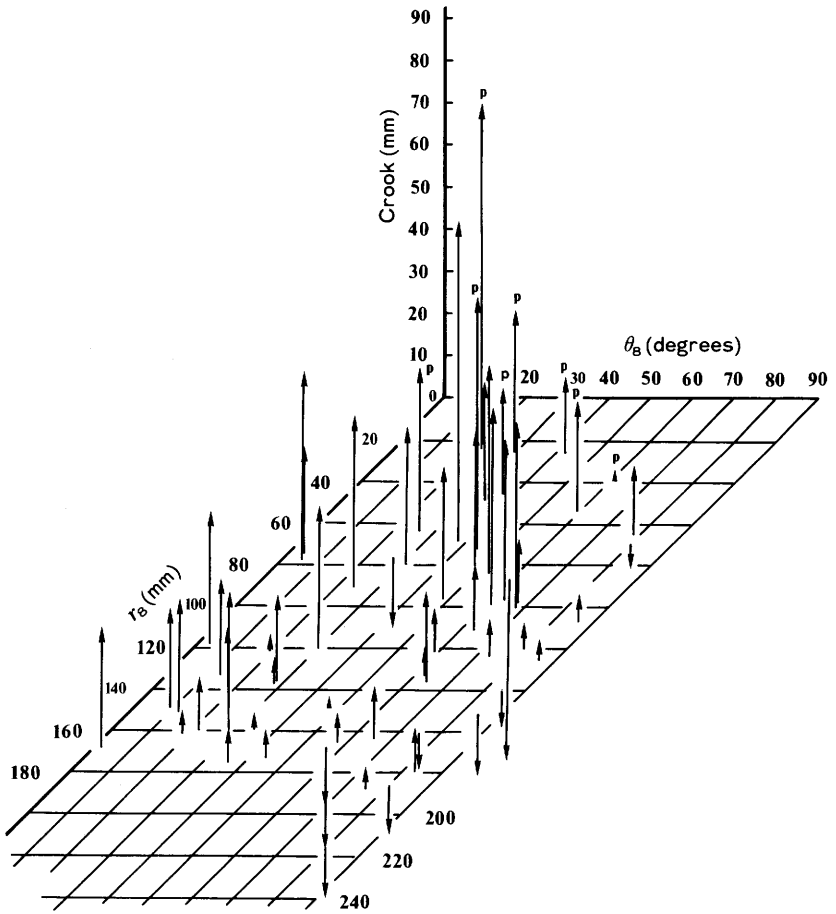

Fig. 43. Relationship between crook and the r_8 and θ_8 coordinates. r_8: average distance from the centroid of the eight cross-sections of each board, as measured by the overlay method. θ_8: average annual ring angle co-ordinate for the eight cross-sections of each board, as measured by the overlay method. P: boards with pith.

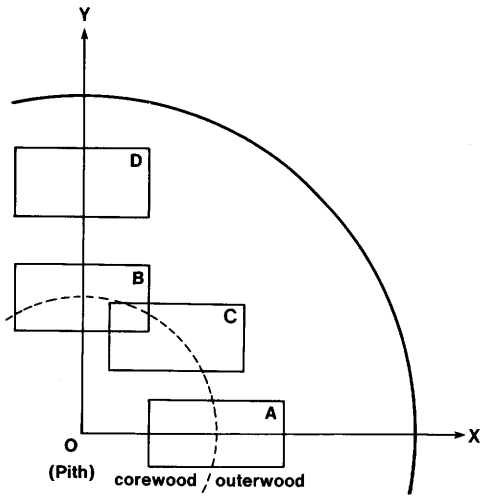

Fig. 44. The effect of the position of the boards with respect to the corewood on bow and crook.

Key words: twist, bow, crook, warping, annual ring orientation, spiral grain, core wood, theory of warp

References

BALODIS, V. 1972: Influence of grain angle on twist in seasoned boards. Wood Science **54**(1): 44–50.

BOOKER, R. E. 1987: A method for recording annual ring orientation in boards. For. Products Journal **37** (6): 31–33.

BS 4978, 1988: Specification for softwood grades for structural use. British Standard 4978.

COWN, D. J. and MCCONCHIE, D. L. 1983(a): Studies on the intrinsic properties of new crop radiata pine 1. Wood characteristics of ten trees from a twelve year old stand grown in the Central North Island. FRI Bulletin No. 36, Forest Research Institute, Private Bag, Rotorua, New Zealand.

COWN, D. J. and MCCONCHIE, D. L. 1983(b): Radiata pine wood properties survey (1977–1982). FRI Bulletin No. 50, Forest Research Institute, Private Bag, Rotorua, New Zealand.

DU TOIT, A. J. 1963: A study of the influence of compression wood on the warping of Pinus radiata D. Don. timber. South African Forestry Journal No. 44: 11–15.

HASLETT, A. N. and MCCONCHIE, D. L. 1986, Commercial utilisation study of radiata pine thinnings for sawn timber production. FRI Bulletin No. 116, Forest Research Institute, Private Bag, Rotorua, New Zealand.

KLOOT, N. H. and PAGE, M. W. 1959: A study of distortion in radiata pine scantlings. Div. of Forest Products Tech. Paper No. 7, CSIRO, Australia.

MACKAY, J F. and RUMBALL, B. L. 1971: Drying of distortion prone juvenile core radiata pine for house studs. Austr. Timber Journal **37**(6): 43–57.

SHELLY, J. R.; ARGANBRIGHT, D. G. and BIRNBACH, M. 1979: Severe warp development in young-growth ponderosa pine studs. Wood and Fiber **11**(1): 50–56.

(Received April 27, 1988)

ニュークロップラジアタパイン2×4材の狂い

三城昭義・ロルフ E. ブッカ

要　旨

ニュークロップラジアタパイン2×4材の乾燥による狂いの性状を明かにするために，生材から含水率約7%まで無拘束で乾燥した時の狂い（縦ぞり，弓ぞり，ねじれ）と狂いに影響するいくつかの因子（材の丸太内における位置，収縮率，繊維傾斜角，比重，節の大きさや分布など）を詳細に調べた。また，狂いの方向をはっきりさせるために leading edge という基準位置を設け，正 (positive) と負 (negative) の縦ぞり，弓ぞりおよびねじれを定義した。2×4材の丸太内における位置は (r, θ) で表し，overlay 法と直接法で測定した（ここで，r は丸太の髄から2×4材の中心までの距離，θ は2×4材の年輪状態を示す値で，0°（柾目板）から90°（板目板）までの範囲にある)。

生材の時は供試材（61本）の約60%が負の縦ぞりおよび弓ぞりを示したが，乾燥すると約80%が正の縦ぞり，弓ぞりを示した。ねじれは繊維傾斜角に強く影響される。

(r, θ) と縦ぞりおよび弓ぞりの3次元のグラフの形は未成熟材と成熟材の繊維方向収縮率の差によって説明できる。縦ぞりは r の値に関係なく，$\theta=0°$（柾目板）の時最大で，$\theta=90°$（板目板）の時最小である。

縦ぞり，弓ぞりおよびねじれとそれぞれの影響因子との関係を調べたが，それぞれの因子はお互いに関連しており，ひとつだけの因子による解析では間違った結果を導くおそれがある。これをさけるためには数学モデルによる解析が必要である。

キーワード：ねじれ，弓ぞり，縦ぞり，年輪傾角，旋回木理，未成熟材，反りの理論